A peer-reviewed version of this preprint was published in PeerJ on 27 October 2017.

View the peer-reviewed version (peerj.com/articles/3965), which is the preferred citable publication unless you specifically need to cite this preprint.

Meneses CS, Müller HY, Herzberg DE, Uberti B, Bustamante HA, Werner MP. 2017. Immunofluorescence characterization of spinal cord dorsal horn microglia and astrocytes in horses. PeerJ 5:e3965
https://doi.org/10.7717/peerj.3965

Immunohistochemical characterization of spinal cord dorsal horn microglia and astrocytes in horses

Constanza Stefania Meneses [1], **Heine Yacob Müller** [1], **Daniel Eduardo Herzberg** [1], **Benjamín Uberti** [2], **Hedie Almagro Bustamante** [2], **Marianne Patricia Werner** Corresp. [3]

[1] Veterinary Sciences Graduate School, Universidad Austral de Chile, Valdivia, Chile
[2] Veterinary Clinical Sciences Department, Universidad Austral de Chile, Valdivia, Chile
[3] Animal Science Department, Universidad Austral de Chile, Valdivia, Chile

Corresponding Author: Marianne Patricia Werner
Email address: marianne.werner@uach.cl

Role of glial cells in pain modulation has recently gathered attention. The objective of this study was to determine healthy spinal microglia and astrocyte morphology and disposition in equine spinal cord dorsal horns using Iba-1 and GFAP/Cx-43 immunofluorescence labeling, respectively. 5 adult horses without visible wounds or gait alterations were selected. Spinal cord segments were obtained post-mortem for immunohistochemical and immunocolocalization assays. Immunodetection of spinal cord dorsal horn astrocytes was done using a polyclonal goat antibody raised against Glial Fibrillary Acidic Protein (GFAP) and a polyclonal rabbit antibody against Connexin 43 (Cx-43). For immunodetection of spinal cord dorsal horn microglia, a polyclonal rabbit antibody against a synthetic peptide corresponding to the C-terminus of ionized calcium-binding adaptor molecule 1 (Iba-1) was used. Epifluorescence and confocal images were obtained for the morphological and organizational analysis. Evaluation of shape, area, cell diameter, cell process length and thickness was performed on dorsal horn microglia and astrocyte. Morphologically, an amoeboid o spherical shape with a mean cell area of 92.4 + 34 µm2 (in lamina I, II and III) was found in horse microglial cells, located primarily in laminae I, II and III. Astrocyte primary stem branches (and cellular bodies to a much lesser extent) are mainly detected using GFAP. Thus, double GFAP/Cx- immunostaining was needed in order to accurately characterize the morphology, dimension and cell density of astrocytes in horses. Horse and rodent astrocytes seem to have similar dimensions and localization. Horse astrocyte cells have an average diameter of 56 + 14 µm, with a main process length of 28 + 8 µm, and thickness of 1.4 + 0.3 µm, mainly situated in laminae I, II and III. Additionally, a close association between end-point astrocyte processes and microglial cell bodies was found. These results are the first characterization of cell morphology and organizational aspects of horse spinal glia. Iba-1 and GFAP/Cx-43 can successfully stain microglia and astrocytes respectively in horse spinal cords, and thus reveal cell morphology and corresponding

distribution within the dorsal horn laminae of healthy horses. The conventional hyper-ramified shape that is normally visible in resting microglial cells was not found in horses. Instead, horse microglial cells had an amoeboid o spherical shape. Horse protoplasmic astroglia is significantly smaller and structurally less complex than human astrocytes, with fewer main GFAP processes. Instead, horse astrocytes tend to be similar to those found in rodent's model, with small somas and large cell processes. Microglia and astrocytes were found in the more superficial regions of the dorsal horn, similarly to that previously observed in humans and rodents. Further studies are needed to demonstrate the molecular mechanisms involved in the neuron-glia interaction in horses.

IMMUNOHISTOCHEMICAL CHARACTERIZATION OF SPINAL CORD DORSAL HORN MICROGLIA AND ASTROCYTES IN HORSES

Constanza Stefania Meneses[3], Heine Yacob Müller[3], Daniel Eduardo Herzberg[3], Benjamín Uberti[2], Hedie Almagro Bustamante[2], Marianne Patricia Werner[1]

[1]Animal Science Department, Universidad Austral de Chile, Valdivia, Chile

[2]Veterinary Clinical Sciences Department, Universidad Austral de Chile, Valdivia, Chile

[3]Veterinary Sciences Graduate School, Universidad Austral de Chile, Valdivia, Chile

Corresponding Author:

Marianne Werner[1]

Independencia 641, Valdivia, 5090000, Chile

Email address: Marianne.werner@uach.cl

ABSTRACT

Background

Role of glial cells in pain modulation has recently gathered attention. The objective of this study was to determine healthy spinal microglia and astrocyte morphology and disposition in equine spinal cord dorsal horns using Iba-1 and GFAP/Cx-43 immunofluorescence labeling, respectively.

Methods

Five adult horses without visible wounds or gait alterations were selected. Spinal cord segments were obtained post-mortem for immunohistochemical and immunocolocalization assays. Immunodetection of spinal cord dorsal horn astrocytes was done using a polyclonal goat antibody raised against Glial Fibrillary Acidic Protein (GFAP) and a polyclonal rabbit antibody against Connexin 43 (Cx-43). For immunodetection of spinal cord dorsal horn microglia, a polyclonal rabbit antibody against a synthetic peptide corresponding to the C-terminus of ionized calcium-binding adaptor molecule 1 (Iba-1) was used. Epifluorescence and confocal images were obtained for the morphological and organizational analysis. Evaluation of shape, area, cell diameter, cell process length and thickness was performed on dorsal horn microglia and astrocyte.

Results

Morphologically, an amoeboid o spherical shape with a mean cell area of 92.4 $\pm$ 34 µm2 (in lamina I, II and III) was found in horse microglial cells, located primarily in laminae I, II and III. Astrocyte primary stem branches (and cellular bodies to a much lesser extent) are mainly detected using GFAP. Thus, double GFAP/Cx-43 immunostaining was needed in order to

accurately characterize the morphology, dimension and cell density of astrocytes in horses. Horse and rodent astrocytes seem to have similar dimensions and localization. Horse astrocyte cells have an average diameter of 56 ± 14 µm, with a main process length of 28 ± 8 µm, and thickness of 1.4 ± 0.3 µm, mainly situated in laminae I, II and III. Additionally, a close association between end-point astrocyte processes and microglial cell bodies was found.

Discussion

These results are the first characterization of cell morphology and organizational aspects of horse spinal glia. Iba-1 and GFAP/Cx-43 can successfully stain microglia and astrocytes respectively in horse spinal cords, and thus reveal cell morphology and corresponding distribution within the dorsal horn laminae of healthy horses. The conventional hyper-ramified shape that is normally visible in resting microglial cells was not found in horses. Instead, horse microglial cells had an amoeboid o spherical shape. Horse protoplasmic astroglia is significantly smaller and structurally less complex than human astrocytes, with fewer main GFAP processes. Instead, horse astrocytes tend to be similar to those found in rodent's model, with small somas and large cell processes. Microglia and astrocytes were found in the more superficial regions of the dorsal horn, similarly to that previously observed in humans and rodents. Further studies are needed to demonstrate the molecular mechanisms involved in the neuron-glia interaction in horses.

Keywords: Microglia, astrocytes, Iba-1, GFAP, Cx-43, horses.

66

67 **INTRODUCTION**

68 Glial cells have historically been considered static constituents of the central nervous system
69 (CNS), displaying functions like support cells for neuronal synapsis, providing neurochemical
70 precursors and energy sources, in addition to regulating the extracellular ionic concentration and
71 removing cellular debris, among others (Haydon, 2001; Watkins et al., 2007). Interestingly, over
72 the past two decades, the role of glial cells in pain modulation has gathered much attention
73 (Gosselin et al., 2010) Scientific evidence has implicated microglia and astrocytes as key cells
74 underlying acute and chronic pain (Hains & Waxman, 2006; Chen et al., 2012). Painful
75 syndromes are associated with glial response that can dynamically modulate the function of CNS
76 neurons, increasing their excitability and reactivity (Temburni & Jakob, 2001). This
77 multifunctionality of glial cells is determined by the activation state of the cell and the
78 components it expresses, which are different in time of action and intensity according to the
79 stimulus that triggers the glial reaction (Watkins et al., 2003). Glial mediators powerfully
80 modulate excitatory and inhibitory synaptic transmission at presynaptic, postsynaptic, and
81 extrasynaptic sites (Ji et al., 2013), and moreover, are involved in the central modifications
82 underlying chronic pain (Gosselin et al., 2010).

83 Painful syndromes trigger a microglial response characterized by the upregulation of specific
84 glial markers such as the ionized calcium-binding adaptor molecule-1 (Iba-1), and/or
85 morphological changes, including hypertrophy, proliferation, and modification of glial networks
86 (Ji et al., 2013). After nerve damage, active microglia display morphological changes, such as
87 switching from ramified to amoeboid shapes (Eriksson et al., 1993) and may show upregulation
88 of Iba-1, a small calcium binding protein specifically expressed by these cells (Hanisch &

89 Kettenmann, 2007). Several studies have demonstrated how Iba-1 is capable of exposing the
90 activation state of microglia according to its morphology (Ito et al., 1998; Faustino et al., 2011).
91 Furthermore, its overexpression is highly correlated with increased nociceptive inputs
92 converging to the dorsal spinal cord days after injury (Yamamoto et al., 2015). Microglial
93 activation seems to frequently occur during the early phase of peripheral or central lesions and
94 may even precede astrocyte changes (Tanga et al., 2004; Hald et al., 2009). Once activated, these
95 cells can release a variety of neuroactive substances, including proinflammatory cytokines (TNF,
96 IL-1, IL-6), nitric oxide (NO), reactive oxygen species (ROS), arachidonic acid products,
97 excitatory amino acids and ATP, increasing the excitability and reactivity of nociceptor neurons
98 (Thameen et al., 2007; Faustino et al., 2011; Yamamoto et al., 2015).

99 Similarly, astrocytic resting and active states have been defined. It is classically considered that
100 resting astrocytes perform a constant housekeeping function, and express basal levels of GFAP
101 (Gosselin et al., 2010). Nevertheless, it appears that initial microglial activation under external
102 stimulation can later lead to astrocyte activation (Tanga et al., 2004). Activation of astrocytes
103 triggers the release of excitatory neuromodulators from the pre-synaptic space that leads to
104 morphological changes, such as cellular hypertrophy and increased GFAP expression, leading to
105 post-translational modifications that allows the secretion of pro-inflammatory substances at the
106 spinal level and ultimately pain hypersensitization (Watkins & Maier, 2005; Hansson, 2006).
107 GFAP is the most widely used and reliable marker for in vivo and in vitro identification of
108 astrocytes (Tomassoni et al., 2004), and represents the mayor component of intermediate
109 filaments in mature astroglia (Brenner, 1994). GFAP has been proven to be important in
110 modulating the motility and shape of astrocytes by giving structural stability to the extensions of
111 cell processes (Eng et al., 2000), in both normal and pathological brain (Bignami et al., 1972),

112 and spinal cord tissues (Song et al., 2016). Despite its high sensitivity, astrocyte labeling is
113 usually accompanied by the detection of another specific marker, called Connexin 43 (Cx-43)
114 (Ochalsky et al., 1996), which is an important component of astrocyte gap junctions that highly
115 coupled these cells (Rouach et al., 2002). Cx-43 maintains the normal shape and function of
116 astrocytes, which is important for their integrity and stability (Wu et al., 2015). After peripheral
117 or central nervous damage, Cx-43 expression markedly increases, and its deletion in astrocytes
118 can reduce acute astrogliosis, and can produce analgesia in different pain models (Gao et al.,
119 2010; Huang et al., 2012).

120 Microglia and astrocyte interaction has been shown to be involved in the establishment and
121 maintenance of pathological states of pain, which after peripheral nerve or spinal damage
122 undergo a physiological and morphological activation in the dorsal horn level (Mika et al, 2013).
123 Several studies suggest that microglia may be temporarily involved in the initiation of pain,
124 while astrocytic activation may be responsible for its long-lasting maintenance (Gosselin et al.,
125 2010). Nevertheless, the exact nature of microglial mediators activating astrocytes and
126 downstream nociceptive pathways remains to be determined. Although it is known that microglia
127 and astrocytes are potential therapeutic targets in pain control, no work has focused on the
128 description of these cells in horses under neither normal conditions nor during painful states. The
129 use of Iba-1, GFAP and Cx-43 in horses has been documented, mainly in encephalic diseases or
130 in embryotic/fetal development studies (Siso et al., 2003; Bielefeldt et al., 2017; Rigoglio et al.,
131 2017). However, an improved understanding of glial cell function and morphology in healthy
132 horses is needed to accurately know what happens in vitro and in vivo in painful syndromes. The
133 objective of this study was to determine healthy spinal microglia and astrocyte morphology and

134 disposition in equine spinal cord dorsal horns using Iba-1 and GFAP/Cx-43 immunofluorescence
135 labeling, respectively.

136

137

138 **MATERIAL AND METHODS**

139 *Animal selection and spinal cord sampling*

140 The Ethics and Bioethic Committee for the Use of Animals in Research of the Universidad
141 Austral de Chile has approved this project (Nº001/2017). Five adult horses (age ≥ 4 years) were
142 selected without distinction of sex, size or breed from a commercial slaughterhouse (Nueva
143 Imperial Ltda., Temuco, Chile) and were evaluated in the holding pen, immediately prior to
144 humane euthanasia by pneumatic stunning and exsanguination, by an equine clinician. Animals
145 with visible wounds, gait alterations (either musculoskeletal or neurological) or other conditions
146 (pregnant, overweight, foal or senior horses) were excluded. Visual gait analysis was done by an
147 experienced equine clinician. Spinal cord tissues were collected immediately after euthanasia.
148 Either cervical spinal segments (C2-C7) or lumbar spinal segments (L1-L6) were sampled and
149 sectioned transversely maintaining the integrity of the segments in their entire continuity and
150 then stored in individual jars containing Bouin fixative (75 mL of saturated aqueous picric acid
151 (1.2% w / v), 25 mL of formalin (40% w/v formaldehyde), and 5 mL of glacial acetic acid). The
152 cranial and caudal aspects of the spinal cord segments were marked using 18G needles.

153 *Histology and immunohistochemistry*

154 Spinal cord segments were fixed for 48 hours in Bouin fixative and then separated into 2 mm
155 thick sections. Briefly, sections were first dehydrated with graded ethanol series (70% to 100%
156 for 1 hour each, plus an extra hour in 100% concentration), then with a mixture of 100% ethanol
157 and pure butanol (1:1) for 1 hour, and finally a dehydration process with pure butanol (two
158 sessions of 1 hour each) was performed. These segments were paraffin-embedded for 4 hours
159 (divided into four separate sessions, 1 hour each at 60°C), to be later sliced into 6 µm sagittal
160 sections using a Jung microtone, and mounted in xylene embedded slides. Each histological
161 section was dewaxed using pure xylene xylol for 10 minutes each, rehydrated in graded series of
162 alcohols (100% to 70%, 5 minutes each) and washed with distilled water. Sections were then
163 treated with sodium citrate buffer (10mM Sodium Citrate, pH 6.0) and microwaved three times
164 for 4 minutes each. All sections were blocked overnight with TCT buffer (carrageenan 0.7%,
165 Triton X-100 0.5% in TBS, pH 7.6) at 4°C. Tissue sections were then rinsed 3 times for 10
166 minutes in Tris-buffered saline (TBS) and incubated with the primary antibody overnight at
167 room temperature (RT). After incubation, tissue sections were washed 3 times for 10 minutes in
168 TBS and incubated with the corresponding secondary antibody for 1 hour. Primary antibody was
169 omitted for negative controls.

170 For immunodetection of spinal protoplasmic astrocytes, a polyclonal goat antibody raised against
171 Glial Fibrillary Acidic Protein (GFAP) (1:50, Santa Cruz Biotechnology, Santa Cruz, CA, USA)
172 and a polyclonal rabbit antibody against Connexin 43 (Cx-43) (1:50, Santa Cruz Biotechnology,
173 Santa Cruz, CA, USA) were used. For immunodetection of spinal microglia, a polyclonal rabbit
174 antibody against a synthetic peptide corresponding to the C-terminus of ionized calcium-binding
175 adaptor molecule 1 (Iba-1) (1:50, Santa Cruz Biotechnology, Santa Cruz, CA, USA) was used.
176 Cx-43 and Iba-1 primary antibodies were conjugated with an Alexa Fluor (labeled either with

488 or 594) (1:500, Invitrogen, Camarillo, CA, USA) goat anti-rabbit secondary antibody for 1 hour at RT. Instead, GFAP primary antibody was conjugated with an Alexa Fluor 488 (1:500, Invitrogen, Camarillo, CA, USA) donkey anti-goat secondary antibody for 1 hour at RT. After immunolabeling, sections were counterstained with DAPI (1:5000, Invitrogen, Camarillo, CA, USA) for 20 minutes at RT, washed with TBS and mounted (Fluorescence Mounting Medium, DAKO).

Double staining immunohistochemistry

Co-localization assays were performed to detect spinal cord dorsal horn grey matter astrocytes and microglia (GFAP and Iba-1), and to confirm astrocyte labeling (GFAP and Cx-43). For double labeling with GFAP and Iba-1, tissue slides were initially processed as previously described, and then incubated separately with a polyclonal goat primary antibody anti-GFAP (1:50, Santa Cruz Biotechnology, Santa Cruz, CA, USA) and a polyclonal rabbit primary antibody anti-Iba-1 (1:50, Santa Cruz Biotechnology, Santa Cruz, CA, USA) overnight at RT, as previously described. The secondary antibodies were incubated sequentially, first with the conjugated anti-goat secondary antibody (Alexa Fluor 488, 1:500, Invitrogen) for 1 hour at RT. After 3 washes with TBS, the conjugated anti-rabbit secondary antibody (Alexa Fluor 594, 1:500, Invitrogen, Camarillo, CA, USA) was incubated for another hour more at RT. Finally, the slides were washed with TBS, counterstained with DAPI (1:5000, Invitrogen, Camarillo, CA, USA) for 20 minutes at RT, washed again with TBS and coverslip mounted. For double labeling with GFAP and Cx-43, tissue slides were incubated separately with a polyclonal goat primary

199 antibody anti-GFAP (1:50, Santa Cruz Biotechnology, Santa Cruz, CA, USA) and a polyclonal
200 rabbit primary antibody anti-Cx-43 (1:50, Santa Cruz Biotechnology, Santa Cruz, CA, USA)
201 overnight at RT. Finally, secondary antibodies were incubated sequentially as described above
202 (Alexa Fluor 488 conjugated anti-goat secondary antibody and Alexa Fluor 594 conjugated anti-
203 rabbit secondary antibody).

204 *Image collection and analysis*

205 Iba-1, GFAP and Cx-43 immunoreactivity were analyzed to evaluate spinal astrocytes and
206 microglia morphology and organization. Stained sections were visualized at 10X, 20X, 40X,
207 60X, 63X and 100X magnifications, and examined using an Eclipse E200 Biological
208 epifluorescence microscope and Olympus FV1000 confocal fluorescent microscope. Images
209 were captured with a Basler Scout scA780-541C camera and collected through Pylon Viewer 4
210 software for epifluorescence microscope images, and laser scanning using Olympus F10
211 Fluorview software for confocal microscope images. Z-stack of optical sections, 0.5 to 0.9 µm in
212 total thickness, was captured from 15 spinal cord tissue slices using a confocal microscope. At
213 10X magnification, an observation of the entire spinal cord was made to select those horses with
214 spinal cord sections that had well defined and completely integrated dorsal horns. Finally, five
215 horses met all requirements and were included in the study.

216 Morphologically, evaluation of shape, area (in spherical form cells) or cell diameter (in hyper-
217 ramified form cells), plus process length and thickness was performed using ImageJ. In the case
218 of microglial cell analysis, Iba-1 positive cells labeled with Alexa Fluor 488 or 594 were
219 considered for this study; for astrocytes, double cell staining with GFAP (Alexa Fluor 488
220 labeled) and Cx-43 (Alexa Fluor 594 labeled) was implemented. The diameter of twenty hyper-
221 ramified cells was determined measuring the longest axis in non-overlapping cells, with a cross

222 sectional line through the nucleus (DAPI marked) and two endpoint branches. A line between the
223 nucleus and the end of a major branch was traced to measure the process length, and the
224 thickness of these cells was defined with a trace line between two parallel sides of the same
225 branch. For spherical form cells, cell surface was defined with the free hand selection tool, and a
226 line around twenty cell bodies was made to calculate the cross sectional area of glial cells.

227 To analyze the distribution of microglial and astrocyte cells at the dorsal horn level, the total
228 number of cells positive to Iba-1, GFAP and Cx-43 at 10X magnification in all dorsal horn
229 sections were counted. First, due to the large size of the horse spinal cord, several photos (2592 x
230 1944 pixels each) were taken to be later reconstructed using Adobe Illustrator CC 2015 software.
231 Using Image J software, cell counting was performed in a defined square perimeter of 1,000 µm2
232 in in three different segments of the dorsal horn (30 random squares per segment), defined as 1)
233 Posterior dorsal horn (including lamina I, II and III), 2) Intermediate dorsal horn (including
234 lamina IV), and 3) Ventral dorsal horn (including lamina V and IV). All data was collected in
235 Microsoft Excel, and means and standard deviations of each previously defined category were
236 obtained.

237

238 **RESULTS**

239 *Morphology and organization of Iba-1 expressing microglia in horse spinal cord dorsal horns*

240 Microglial cells labeling using Iba-1 was accomplished in all horses. Microglia showed a
241 spherical or amoeboid shape (Fig. 1A to D), with a mean cell area of 92.4 $\pm$ 34 µm2. Within the
242 dorsal horn, Iba-1 fluorescence varied in all study subjects. At 10X magnification, the
243 distribution of Iba-1 microglial cells varied among areas within the dorsal horn from the same

244 horse. The higher number of Iba-1 positive cells were found in the posterior dorsal horn, equally
245 reactive in both dorsal horns (Fig. 1E). In all horses, the average number of microglial cells was
246 9.4 ± 1.8 cells for the posterior dorsal horn, 3.8 ± 3.1 cells for the intermediate dorsal horn, and
247 2.5 ± 2.0 cells for the ventral dorsal horn. Additionally, a close association between microglia
248 and astrocytes processes was observed using Iba-1 and GFAP double immunostaining (Fig. 2A),
249 mainly between microglial cell bodies and secondary astrocyte branches.

250 *Morphology and organization of GFAP and Cx-43 expressing protoplasmic astrocytes in horse*
251 *spinal cord dorsal horns*

252 Astrocytes were successfully detected and characterized using GFAP and Cx-43. GFAP was
253 mainly found in astrocytic primary processes, demonstrating a hyper-ramified cell shape with
254 small somas (Fig. 2C). Also, primary astrocyte processes extend to 2 - 4 long branches, with a
255 mean of 2 small thin branches arising from the main one, often found in association with
256 neighboring astrocytes and microglia (Fig. 2A), in addition to adjacent blood vessels (Fig. 2B)
257 and neurons (Fig. 2C). The arising small branches were only visualized using confocal images in
258 Z projection. Double immunofluorescence with GFAP and Cx-43 was needed to better define
259 astrocyte cell bodies and extensions of processes (Fig. 2D and E). According to GFAP and Cx-
260 43 co-localization assays, horse astrocytes have an average diameter of 56 ± 14 µm, with a main
261 process length of 28 ± 8 µm, and thickness of 1.4 + 0.3 µm. Since it was not possible to visualize
262 the complete cell size at 10X magnification using only GFAP, the cellular density of astrocytes
263 was defined using double staining with Cx-43. Astrocyte cells were distributed throughout all
264 laminae with a high, moderate and minimal fluorescence. The average number of cells in each
265 segment was: 6.1 ± 2.0 cells for the posterior dorsal horn, 3.6 ± 1.2 cells for the intermediate
266 dorsal horn, and 1.6 ± 1.0 cell for the ventral dorsal horn. Astrocytes were found in cell

267 agglomerations along with other astrocytes, with minimal contact between other groups and a
268 tight connection between end-point processes and capillary walls (Fig. 2F).

269

270 **DISCUSSION**

271 It is well known that microglia and astrocytes are potential therapeutic targets for pain control.
272 Therefore, it becomes necessary to understand how these cells maintain and modulate CNS
273 homeostasis (Old et al., 2015). Several studies have generated a list of glial-derived signaling
274 molecules and mediators involved in the neuron-glia interaction in acute and chronic states of
275 pain (Ji et al., 2013). Despite this, there is still a gap in our knowledge about how glial cells are
276 able to alter and maintain states of central sensitization, and even more, mask the analgesic
277 effects of opioids in chronic exposures (Watkins et al., 2007; Old et al., 2015). Until now, the
278 study and detection of these cells has been based on the use of immunomarkers, and of all of
279 them, Iba-1 and GFAP/Cx-43 have been essential to identify microglia and astrocytes,
280 respectively, using immunohistochemical, immunoblotting (Western blot analysis) and RT-PCR
281 assays, in both in clinical and basic neurobiological studies (Tetzlaff et al., 1988; Eng et al, 2000;
282 Tomassoni et al., 2004).

283 *Spinal microglial cells in the dorsal horn of healthy horses*

284 In this study, we demonstrated that Iba-1 can successfully stain microglial cells in horse spinal
285 cords, and thus reveal microglia morphology and corresponding distribution within the dorsal
286 horn laminae of healthy horses. Horse microglial cells had an amoeboid o spherical shape (Fig.
287 1A to D), located in the same site as in rodents (Zhang et al., 2008), in lamina I, II and III (Fig.
288 1E). Nevertheless, the conventional hyper-ramified shape that is normally visible in resting

289 microglial cells (Ito et al., 1998) was not found in any subject. Typically, an amoeboid shape
290 represents active or overactive states of microglial cells after nerve damage (Eriksson et al.,
291 1993). Regardless of this, recent studies have shown that microglia´s morphological
292 characterization is more flexible and dynamic than previously described, and microglial cell
293 morphology can range from ramified cells to hypertrophied cells with large somas, both in
294 resting or active states (Zhang et al., 2008; Nimmerjahn et al., 2015). A recent study reported
295 that encephalitic diseases in horses induce an intense branching appearance of microglial cells
296 (Bielefeldt-Ohmann et al., 2017). Therefore, there is no evidence that microglial cells in horses
297 have a determined phenotype in both pathological o healthy conditions. This information is
298 extremely valuable when looking for the prototypic phenotype of microglial cells in horses and
299 should be considered. Apparently, the general concept that different states of health can frame a
300 specific cellular form does not exist in horses, just as it has been proven in rodents, evidencing
301 that more than one type of morphology may be found, and thus, microglial morphology does not
302 necessarily imply specific functionality.

303 *Spinal astrocytes in the dorsal horn of healthy horses*

304 GFAP has been extensively used as an astrocyte marker in several mammalian species in
305 addition to humans and rodents (Machado & Alessi, 1997; Nielsen & Jørgensen, 2003; Toda et
306 al., 2007; Sikasunge et al., 2009). However, there are no morphological nor structural
307 descriptions of astrocytes in equine spinal cord grey matter. In our study, we demonstrated that
308 GFAP and Cx-43 can successfully immunostain spinal astrocytes in horses, and additionally
309 reveal the morphology and organization of these cells in healthy conditions, although the
310 complete mapping of astrocytes´ structure is quite complicated for several reasons. GFAP is not
311 present throughout the astrocyte cytoplasm, and does not label all portions of the cell; it is mostly

312 expressed in primary stem branches, and to a much lesser extent in the cellular bodies (Bushong
313 et al., 2002, Blechingberg et al., 2007). Therefore, to properly define astrocyte cell structure,
314 double immunostaining of GFAP along with another astrocyte specific marker was necessary. As
315 in other studies, co-localization with Cx-43 permitted accurate characterization of the
316 morphology, dimension and cell density of astrocytes in horses (Fig. 2D and E).

317 According to these findings, horse protoplasmic astroglia is significantly smaller and structurally
318 less complex than human astrocytes (Oberheim et al., 2009), with fewer main GFAP processes.
319 Instead, horse astrocytes tend to be similar to those found in rodent's models. In terms of cell
320 measurements, we observed that horse astrocytes had an average diameter of 56.0 $\pm$ 14 µm, with
321 a main process length of 28.0 $\pm$ 8 µm and thickness of 1.4 $\pm$ 0.3 µm. These same measurements
322 in rodents are 56.0 $\pm$ 2.0 µm, 37.2 $\pm$ 2.0 µm and 2.2 $\pm$ 0.13 µm, respectively (Oberheim et al.,
323 2009). Therefore, horse and rodent astrocytes seem to have similar cell dimensions, considerably
324 different to those in humans (142.6 $\pm$ 5.8 µm, 97.9 $\pm$ 5.2 µm and 2.9 $\pm$ 0.18 µm, respectively
325 (Oberheim et al., 2009)).

326 Like rodents, horse astrocytes are mainly located in laminae I, II and III (Ochalski et al., 1996).
327 Several studies in humans and rodents explain that spinal astrocytes are organized into domains,
328 where each cell occupies its own anatomical space surrounding a neuronal synaptic space, with
329 process projections that penetrate the process-delimited domains of only a single neighboring
330 astrocyte (Oberheim et al., 2008). In this study, we showed that horse astrocytes have a defined
331 group of cells (Fig. 2F), with minimal contact between other groups and a stretch connection
332 between end-point processes and other astrocytes, microglial cells, neurons and capillaries (Fig.
333 2A to C). So far, there is accumulating evidence that the neuron-glia-blood interaction at the
334 spinal cord dorsal horn level is the basis for inter- and intra-cellular signaling mechanisms that

influence synaptic activity and cell growth and nutrition, in addition to pain signaling that contribute to exacerbate chronic and neuropathological pain (Milligan & Watkins, 2009; Sofroniew, 2009; Sofroniew & Vinters, 2010). Nevertheless, more studies are needed to demonstrate the molecular mechanisms involved in the neuron-glia interaction in horses.

CONCLUSIONS

Although rodents have increased our understanding of pain mechanisms and help predict the effectiveness of certain analgesic mechanisms (Whiteside et al., 2008), our knowledge of the molecular and cellular mechanisms that underlie chronic pain remains substantially incomplete. Several authors have demonstrated that there are significant differences in the metabolism and anatomy of rodents that can affect extrapolation of data to humans (Mogil et al., 2010). Future research should focus in the development of improved animal models, to investigate the role of glial cells in central sensitization and persistent pain in a more adequate temporal-spatial circumstance. The results described here, including shape, cell dimension and distribution within the dorsal horn of microglia and astrocytes in healthy horses, characterize for the first time the morphology and organizational aspects of horse spinal glia. To our knowledge, this morphologic cell type has not been described before in healthy horse dorsal horns through immunofluorescence assays, and is more similar in morphology and organization to rodent than human tissue samples. We believe that a clear understanding of the molecular mechanisms underlying horse glial function is necessary, and could represent a novel approach for efficient novel pharmacological targeting. Upcoming studies will address the molecular and cellular modifications in the neuron-glia network under acute and chronic painful conditions in horses.

357

358 **ACKNOWLEDGEMENTS**

359 We gratefully thank Genaro Alvial (Research Assistant at Faculty of Medicine, Universidad
360 Austral de Chile) for his technical support in immunohistochemical analysis.

361

362

363

364

365

366

367 **REFERENCES**

368 Bielefeldt-Ohmann H, Bosco-Lauth A, Hartwig AE, Uddin MJ, Barcelon J, Suen WW, Wang W,
369 Hall RA, Bowen RA. 2017. Characterization of non-lethal West Nile Virus (WNV) infection in
370 horses: Subclinical pathology and innate immune response. Microbial Pathogenesis 103: 71-79.

371 Bignami A, Eng LF, Dahl D, Uyeda CT. 1972. Localization of the glial fibrillary acidic protein
372 in astrocytes by immunofluorescence. Brain Research 43: 429-435.

373 Blechingberg J, Holm IE, Nielsen KB, Jensen TH, Jorgensen AL, Nielsen AL. 2007.
374 Identification and characterization of GFAPkappa, a novel glial fibrillary acidic protein isoform.
375 Glia 55: 497-507.

376 Brenner M. 1994. Structure and transcriptional regulation of the GFAP gene. Brain Pathology 4:
377 245-257.

378 Bushong EA, Martone MA, Jones YZ, Ellisman MH. 2002. Protoplasmic astrocytes in CA1
379 atratum radiatum occupy separate anatomical domains. Journal of Neuroscience 22: 183-192.

380 Chen MJ, Kress B, Han X, Moll K, Peng W, Ji RR, Nedergaard M. 2012. Astrocytic CX43
381 hemichannels and gap junctions play a crucial role in development of chronic neuropathic pain
382 following spinal cord injury. Glia 60: 1660-1670.

383 Eng LF, Ghirnikar RS, Lee YL. 2000. Glial fibrillary acidic protein: GFAP-thirty-one years
384 (1969–2000). Neurochemical Research 25: 1439-1451.

385 Eriksson NP, Persson JK, Svensson M, Arvidsson J, Molander C, Aldskogius H. 1993. A
386 quantitative analysis of the microglial cell reaction in central primary sensory projection
387 territories following peripheral nerve injury in the adult rat. Experimental Brain Research 96: 19-
388 27.

389 Faustino JV, Wang X, Johnson CE, Klibanov A, Derugin N, Wendland MF, Vexler ZS. 2011.
390 Microglial cells contribute to endogenous brain defenses after acute neonatal focal stroke.
391 Journal of Neuroscience Research 31: 12992-13001.

392 Gao YJ, Ji RR. 2010. Targeting astrocyte signaling for chronic pain. Neurotherapeutics 7: 482-
393 493.

394 Gosselin RD, Suter M, Ji RR, Decosterd I. 2010. Glial cells and chronic pain. Neuroscientist 16:
395 519-531.

396 Hains BC, Waxman SG. 2006. Activated microglia contribute to the maintenance of chronic pain
397 after spinal cord injury. Journal of Neuroscience 26: 4308-4317.

398 Hald A, Nedergaard S, Hansen RR, Ding M, Heegaard AM. 2009. Differential activation of
399 spinal cord glial cells in murine models of neuropathic and cancer pain. European Journal of Pain
400 13: 138-145.

401 Hanisch UK, Kettenmann H. 2007. Microglia: active sensor and versatile effector cells in the
402 normal and pathologic brain. Nature Neuroscience 10: 1387-1394.

403 Hansson E. 2006. Could chronic pain and spread of pain sensation be induced and maintained by
404 glial activation? Acta Physiologica 187: 321-327.

405 Haydon PG. 2001. Glia: listening and talking to the synapse. Nature Reviews Neuroscience 2:
406 185-193.

407 Huang C, Han X, Li X, Lam E, Peng W, Lou N, Torres A, Yang M, Garre JM, Tian GF, Bennett
408 M, Nedergaard M, Takano T. 2012. Critical role of connexin 43 in secondary expansion of
409 traumatic spinal cord injury. Journal of Neuroscience 32: 3333-3338.

410 Ito D, Imai Y, Ohsawa K, Nakajima K, Fukuuchi Y, Kohsaka S. 1998. Microglia-specific
411 localisation of a novel calcium binding protein, Iba1. Molecular Brain Research 57: 1-9.

412 Ji RR, Berta T, Nedergaard M. 2013. Glia and pain: is chronic pain a gliopathy? Pain 154: 10-28.

413 Machado GF, Alessi AC. 1997. Glial fibrillary acidic protein (GFAP) immunoreactive astrocytes
414 in the CNS of normal and rabies-infected adult cattle. I. Hippocampus and dentate gyrus.
415 Brazilian Journal of Veterinary Research and Animal Science 34: 345-348.

416 Mika J, Zychowska M, Popiolek-Barczyk K, Rojewska E, Przewlocka B. 2013. Importance of
417 glial activation in neuropathic pain. European Journal of Pharmacology 716: 106-119.

418 Milligan ED, Watkins LR. 2009. Pathological and protective roles of glia in chronic pain. Nature
419 Reviews Neuroscience 10: 23-36.

420 Mogil JS, Davis KD, Derbyshire SW. 2010. The necessity of animal models in pain research.
421 Pain 151: 12-17.

422 Nielsen AL, Jørgensen AL. 2003. Structural and functional characterization of the zebrafish gene
423 for glial fibrillary acidic protein, GFAP. Gene 310: 123-132.

424 Nimmerjahn A, Kirchhoff F, Helmchen F. 2005. Resting microglial cells are highly dynamic
425 surveillants of brain parenchyma in vivo. Science 308: 1314-1318.

426 Oberheim NA, Takano T, Han X, He W, Lin JH, Wang F, Xu Q, Wyatt JD, Pilcher W, Ojemann
427 JG, Ransom BR, Goldman SA, Nedergaard M. 2009. Uniquely hominid features of adult human
428 astrocytes. Journal of Neuroscience 29: 3276-3287.

429 Oberheim NA, Tian GF, Han X, Peng W, Takano T, Ransom B, Nedergaard M. 2008. Loss of
430 astrocytic domain organization in the epileptic brain. Journal of Neuroscience 28: 3264-3276.

431 Ochalski P, Frankenstein UN, Hertzberg EL, Nagy JI. 1996. Connexin-43 in rat spinal cord:
432 localization in astrocytes and identification of heterotypic astro-oligodendrocytic gap junctions.
433 Neuroscience 76: 931-945.

434 Old EA, Clark AK, Malcangio M. 2015. The role of glia in the spinal cord in neuropathic and
435 inflammatory pain. In: Schaible HG, ed. Pain Control. Berlin: Springer Berlin Heidelberg, 145-
436 170.

437 Rigoglio NN, Barreto RS, Favaron PO, Jacob JC, Smith LC, Gastal MO, Gastal E, Miglino MA.
438 2017. Central Nervous System and Vertebrae Development in Horses: A Chronological Study
439 with Differential Temporal Expression of Nestin and GFAP. Journal of Molecular Neuroscience
440 61: 61-78.

441 Rouach N, Avignone E, Même W, Koulakoff A, Venance L, Blomstrand F, Giaume C. 2002.
442 Gap junctions and connexin expression in the normal and pathological central nervous system.
443 Biologie Cellulaire 94: 457-475.

444 Sikasunge CS, Johansen MV, Phiri IK, Willingham AL, Leifsson PS. 2009. The immune
445 response in Taenia solium neurocysticercosis in pigs is associated with astrogliosis, axonal
446 degeneration and altered blood–brain barrier permeability. Veterinary Parasitology 160: 242-
447 250.

448 Siso S, Ferrer I, Pumarola M. 2003. Abnormal synaptic protein expression in two Arabian horses
449 with equine degenerative myeloencephalopathy. Veterinary Journal 166: 238-243.

450 Sofroniew MV, Vinters HV. 2010. Astrocytes: biology and pathology. Acta Neuropathologica
451 119: 7-35.

452 Sofroniew MV. 2009. Molecular dissection of reactive astrogliosis and glial scar formation.
453 Trends in Neurosciences 32: 638-647.

454 Song ZP, Xiong BR, Guan XH, Cao F, Manyande A, Zhoun Y, Xheng H, Tian Y. 2016.
455 Minocycline attenuates bone cancer pain in rats by inhibiting NF-kB in spinal astrocytes. Acta
456 Pharmacologica Sinica 37: 753-762.

457 Tanga FY, Raghavendra V, DeLeo JA. 2004. Quantitative realtime RT-PCR assessment of spinal
458 microglial and astrocytic activation markers in a rat model of neuropathic pain. Neurochemistry
459 International 45: 397-407.

460 Temburni MK, Jacob MH. 2001. New functions for glia in the brain. Proceedings of the National
461 Academy of Sciences 98: 3631-3632.

462 Tetzlaff W, Graeber MB, Bisby MA, Kreutzberg GW. 1988. Increased glial fibrillary acidic
463 protein synthesis in astrocytes during retrograde reaction of the rat facial nucleus. Glia 1: 90-95.

464 Thameem DS, Kaur C, Ling EA. 2007. Microglial activation and its implications in the brain
465 diseases. Current Medicinal Chemistry 14: 1189-1197.

466 Toda Y, Matsuki N, Shibuya M, Fujioka I, Tamahara S, Ono K. 2007. Glial fibrillary acidic
467 protein (GFAP) and anti-GFAP autoantibody in canine necrotising meningoencephalitis.
468 Veterinary Record 161: 261-264.

469 Tomassoni D, Avola R, Di Tullio MA, Sabbatini M, Vitaioli L, Amenta F. 2004. Increased
470 expression of glial fibrillary acidic protein in the brain of spontaneously hypertensive rats.
471 Clinical and Experimental Hypertension 26: 335-350.

472 Watkins LR, Hutchinson MR, Ledeboer A, Wieseler-Frank J, Milligan ED, Maier SF. 2007. Glia
473 as the "bad guys": implications for improving clinical pain control and the clínical utility of
474 opioids. Brain Behavior and Immunity 21: 131-146.

475 Watkins LR, Maier SF. 2005. Immune regulation of central nervous system functions: from
476 sickness responses to pathological pain. Journal of Internal Medicine 257: 139-155.

477 Watkins LR, Milligan ED, Maier SF. 2005. Glial proinflammatory cytokines mediate
478 exaggerated pain states: implications for clinical pain. Advances in Experimental Medicine and
479 Biology 521: 1-21.

480 Whiteside GT, Adedoyin A, Leventhal L. 2008. Predictive validity of animal pain models? A
481 comparison of the pharmacokinetic–pharmacodynamic relationship for pain drugs in rats and
482 humans. Neuropharmacology 54: 767-775.

483 Wu LY, Yu XL, Feng LY. 2015. Connexin 43 stabilizes astrocytes in a stroke-like milieu to
484 facilitate neuronal recovery. Acta Pharmacologica Sinica 36: 928-938.

485 Yamamoto Y, Terayama R, Kishimoto N, Maruhama K, Mizutani M, Iida S, Sugimoto T. 2015.
486 Activated microglia contribute to convergent nociceptive inputs to spinal dorsal horn neurons
487 and the development of neuropathic pain. Neurochemical Research 40: 1000-1012.

488 Zhang F, Vadakkan KI, Kim SS, Wu LJ, Shang Y, Zhuo M. 2008. Selective activation of
489 microglia in spinal cord but not higher cortical regions following nerve injury in adult mouse.
490 Molecular Pain 4: 15-31.

491

Figure 1

Microglial immunostaining against Iba-1 in equine spinal cord dorsal horns

Microglial immunostaining against Iba-1 in equine spinal cord dorsal horns (Iba-1, green; DAPI, blue). Microglia showed a spherical or amoeboid shape, constantly throughout the dorsal horn (63X magnification, epifluorescence microscopy) (A, B, C and D). Distribution of Iba-1 marked microglia varied in different areas of the dorsal horn, with a higher microglial cell population in the posterior dorsal horn (*i.e.* laminae I, II and III) (10X magnification, epifluorescence microscopy) (E). Scale bar, 20 µm (n=5).

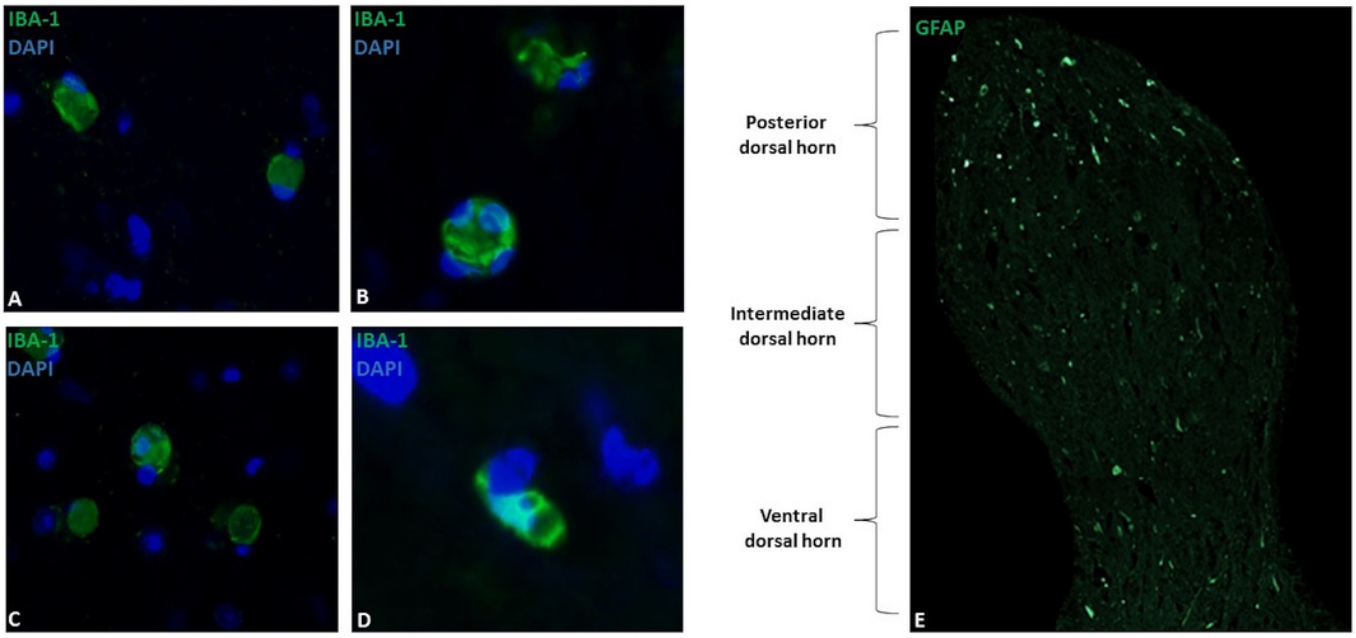

Figure 2

Representative epifluorescence and confocal images of longitudinal sections of spinal cord dorsal horn in healthy horses

Representative epifluorescence and confocal images of longitudinal sections of spinal cord dorsal horn in healthy horses. The sections were doubly immunolabeled against GFAP (green), Cx-43 (red) and DAPI (blue) to detect astrocytes, and doubly immunolabeled against GFAP (green), Iba-1 (red) and DAPI (blue) to detect astrocytes and microglial cells. Astrocytes have increased GFAP expression towards the end of their feet processes, and the thin branches arising from the primary processes were in close contact with neighboring astrocytes and microglia (A), vessels (B; bv) and neurons (C; white arrow). Cx-43 was located in cell bodies (D) and processes (E), and astrocytes were found in cell agglomerations along with other astrocytes (F). Images at 60X magnification, scale bar 20 µm (n=5).